IOPscience iopscience.iop.org

Home Search Collections Journals About Contact us My IOPscience

Photoluminescence of n-type $CdGeAs_2$

This article has been downloaded from IOPscience. Please scroll down to see the full text article.

2005 J. Phys.: Condens. Matter 17 5687

(http://iopscience.iop.org/0953-8984/17/37/007)

View the table of contents for this issue, or go to the journal homepage for more

Download details:
IP Address: 129.252.86.83
The article was downloaded on 28/05/2010 at 05:57

Please note that terms and conditions apply.

INSTITUTE OF PHYSICS PUBLISHING JOURNAL OF PHYSICS: CONDENSED MATTER

J. Phys.: Condens. Matter **17** (2005) 5687–5696 doi:10.1088/0953-8984/17/37/007

Photoluminescence of n-type $CdGeAs_2$

Lihua Bai[1], Chunchuan Xu[1], K Nagashio[2,4], Chunhui Yang[2,5], R S Feigelson[2], P G Schunemann[3] and N C Giles[1,6]

[1] Physics Department, West Virginia University, Morgantown, WV 26506, USA
[2] Geballe Lab for Advanced Materials, Stanford University, Stanford, CA 94305, USA
[3] BAE Systems, Nashua, NH 03061, USA

E-mail: Nancy.Giles@mail.wvu.edu

Received 27 April 2005, in final form 8 August 2005
Published 2 September 2005
Online at stacks.iop.org/JPhysCM/17/5687

Abstract
Samples of n-type $CdGeAs_2$ were produced by intentional doping with indium, selenium, or tellurium impurities. A near-edge photoluminescence (PL) band from heavily In-doped $CdGeAs_2$ samples shifts to higher energy and becomes broader with increasing electron concentration. The observed shifts in peak energies are compared to predictions for donor–acceptor pair and free-to-bound (electron–acceptor) recombinations including band filling, band tailing, and band gap shrinkage effects due to the high doping levels. For $n > 2\times10^{18}$ cm^{-3}, the free-to-bound PL transition related to a shallow 120 meV acceptor level is dominant. A lower energy PL band due to deep acceptors and normally seen for p-type samples is the only emission observed from less n-type samples ($n \sim 10^{16}$–10^{17} cm^{-3}) doped with indium, selenium, or tellurium impurities. Transitions involving the deep acceptor level are not present in the PL for heavily In-doped $CdGeAs_2$ crystals, which suggests that the deep acceptor may be a Cd vacancy.

1. Introduction

$CdGeAs_2$ is a direct band gap II–IV–V_2 ternary chalcopyrite that has sufficient birefringence and a large nonlinear electro-optic coefficient, which makes it suitable for use in infrared frequency conversion applications. The band gap of this material is about 0.57 eV [1] at room temperature and about 0.67 eV [2] at liquid helium temperature. In recent years, large, crack-free, single crystals have been grown by the horizontal gradient freeze (HGF) technique [3–6]. Although laser devices have been reported using $CdGeAs_2$ crystals, absorption losses due to defects are still a major limitation for the efficiency of the devices [7–10].

[4] Present address: Japan Aerospace Exploration Agency, Sagamihara, Kanagawa, Japan.
[5] Present address: Department of Applied Chemistry, Harbin Institute of Technology, 150001, People's Republic of China.
[6] Author to whom any correspondence should be addressed.

 © 2005 IOP Publishing Ltd Printed in the UK

As-grown $CdGeAs_2$ crystals grown by the HGF technique are usually p-type. Several absorption bands extend from the band edge near 2.3 μm out to 8 μm. These absorption bands have been assigned to transitions involving two acceptors (one deep and one shallow) and one donor [11]. A discrete absorption band at 5.5 μm for p-type material is assigned to the intervalence band transition [12] between the top two valence bands resulting from free holes created by thermal ionization of the acceptors. This 5.5 μm band is easily observed at 300 K for p-type material. Two photoluminescence (PL) bands are also generally seen for p-type $CdGeAs_2$ crystals [13–15]. One broad PL band peaking near 0.35 eV is present for most p-type samples. This band was assigned to a donor–acceptor pair (DAP) recombination involving a shallow 14 meV donor and a deep 260 meV acceptor [11, 13, 15]. The other commonly seen PL band for p-type $CdGeAs_2$ occurs near 0.55 eV, is present for samples with enhanced 5.5 μm absorption, and is attributed to a DAP recombination involving shallow donors and a shallow 120 meV acceptor [13–15]. The 0.55 eV DAP emission can vary in peak position by tens of meV due to potential fluctuations caused by high concentrations of defects in as-grown material [16]. The shallow acceptor has been tentatively assigned to a Ge_{As} antisite defect, on the basis of electron paramagnetic resonance [17] and supported by theoretical predictions [18].

Intentional doping of $CdGeAs_2$ crystals with donor impurities can provide compensation of acceptors and lead to reduction of the unwanted 5.5 μm absorption band. However, too high a donor doping level is just as detrimental to the optical device performance, since free carrier absorption will be present. Indium, selenium, and tellurium have been used as substitutional donors to provide n-type $CdGeAs_2$ material [19, 20]. Not much is known about the specific defect levels produced by these impurities, or how they interact with the native acceptors commonly observed in the as-grown p-type material. Indium is expected to incorporate on the group II site in $CdGeAs_2$ and behave as a singly ionized shallow donor. Indium doping has often been used to produce n-type behaviour for II–VI compounds, and the indium ions are closely matched to Cd ions in size. Selenium and tellurium are expected to incorporate on the group V anion site (the As site) in order to behave as singly ionized donors. In this paper, the PL of n-type $CdGeAs_2$ samples doped with indium, selenium, or tellurium is reported and an analysis of peak shifts with increasing electron concentration in In-doped samples is presented. The PL data provide a determination of which acceptor levels are present in these n-type crystals.

2. Experiment set-up

The $CdGeAs_2$ samples used in this investigation were grown by the HGF technique at Stanford University and at BAE Systems. Data from 12 samples cut from five different boules are described here. The sample sizes were (4–5) $\times$ (3–5) $\times$ (0.6–1.8) mm^3. Table 1 provides a summary of the boule and sample characteristics. The doping levels indicate the relative impurity amounts added to the melt. The three indium-doped boules included in our study were grown with approximately 10, 100, and 1000 ppm of In. The 1000 ppm In boule was grown along the [001] direction and samples cut from different locations along the growth direction had 300 K free electron concentrations varying by one order of magnitude. The 1000 ppm doping level would correspond to approximately 2×10^{19} cm^{-3} if complete and uniform incorporation and activation of the donor dopant occurred with no compensation of acceptor states. The In-doped boule grown along the [112] direction with 100 ppm of indium yielded more uniform results and samples exhibited free electron concentrations close to predicted levels for complete and uniform incorporation. For doping with 10 ppm In, or with Se or Te, there were regions in the boules which still exhibited p-type conductivity at 300 K. The twelve

Table 1. Summary of impurity doping levels and Hall data (carrier concentrations and mobilities) for the twelve n-type $CdGeAs_2$ samples included in our study. The doping levels indicate the relative amounts of impurity atoms which were added to the melt.

Boule growth direction	Sample	Impurity, doping level	Electron concentration n (cm^{-3})	Electron mobility μ ($cm^2\ V^{-1}\ s^{-1}$)
[001][a]	a	In, 1000 ppm	4.3×10^{18}	1030
[001][a]	b	In, 1000 ppm	2.7×10^{18}	974
[001][a]	c	In, 1000 ppm	4.6×10^{17}	199
[112][b]	d	In, 100 ppm	2.9×10^{18}	987
[112][b]	e	In, 100 ppm	1.9×10^{18}	1390
[112][b]	f	In, 100 ppm	1.8×10^{18}	1490
[112][b]	g	In, 100 ppm	1.6×10^{18}	1360
[112][b]	h	In, 100 ppm	1.5×10^{18}	1430
[112][b]	i	In, 10 ppm	3.3×10^{17}	2040
[112][b]	j	In, 10 ppm	2.3×10^{17}	2770
[112][b]	k	Te, 500 ppm	1.4×10^{17}	1150
[001][a]	l	Se, 1000 ppm	8.8×10^{16}	1640

[a] Grown at BAE Systems.
[b] Grown at Stanford University.

n-type samples selected for this PL study were oriented and cut with the c direction (i.e. the [001] direction) perpendicular to the surfaces used for the optical measurements. Sample surfaces were mechanically polished using diamond paste with granulation down to 0.1 μm. Prior work has shown that surfaces prepared in this way are suitable for PL experiments [15]. Hall-effect measurements were performed using indium solder contacts in a van der Pauw geometry and a commercial system from MMR Technologies.

PL spectra were acquired using a nitrogen-purged Fourier-transform infrared (FTIR) spectrometer (ThermoNicolet Nexus 870). A CaF_2 beam splitter and a cooled HgCdTe detector were used to take the data. Samples were mounted in an Oxford Instruments cryostat (helium gas flow system) positioned outside the FTIR. This allowed the sample temperature to be maintained near 10 K during the measurements. A Nd:YAG laser operating at 1.064 μm (1.17 eV) was used as an above-band-gap cw excitation source. The incident power density of the laser beam on the sample was about 7.6 W cm^{-2} unless stated otherwise. Emitted light from the sample was collected by a CaF_2 lens and directed into the FTIR spectrometer through an external port. Scattered laser light was blocked by a polished Ge wafer placed in the optical path and used as a long-pass filter. An optical chopper and lock-in amplifier allowed detection of the PL signal portion of the interferogram provided by the internal HgCdTe detector of the FTIR system.

3. Results and discussion

PL data from the indium-doped $CdGeAs_2$ samples will be described first. Figure 1 shows spectra taken at 10 K from samples a, b, and c. The higher energy emission bands from these three samples are centred near 0.63, 0.61, and 0.51 eV, respectively. For samples a and b, the lower energy PL band peaking near 0.35 eV is absent, although a weak emission from 0.4 to 0.5 eV is seen for sample b. The PL from samples cut from the 100 ppm boule (samples d–h) were similar to those obtained from samples a and b, in that the commonly observed 0.35 eV emission is absent and the spectra are dominated by a broad near-edge PL band near 0.6 eV or

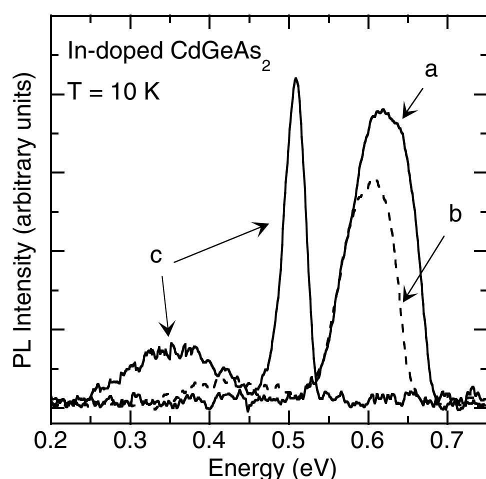

Figure 1. PL spectra taken at 10 K for three n-type In-doped $CdGeAs_2$ samples: sample a (solid line), sample b (dotted line), and sample c (solid line).

higher. It is interesting that incorporation of high levels of In donors has reduced or eliminated the radiative recombination involving the deep acceptor associated with the 0.35 eV PL band. In contrast, the PL from sample c shows two bands and is similar to PL spectra observed from p-type samples having the two acceptors [15]. Sample c has the lowest Hall mobility for our sample set. The differences in PL behaviour depicted in figure 1 (samples cut from the same boule) may be partially explained by the typical variations in optical uniformity that have been reported for undoped $CdGeAs_2$ bulk crystals [6, 21]. Cross-sections cut normal to the growth direction typically exhibit distinct regions of different optical transparency, and preferential incorporation of impurities, structural defects (dislocations), and native defects (acceptors) may occur for certain faceted planes [6]. For these intentionally doped samples, impurity segregation along the growth direction may also be a factor.

The PL bands observed for $CdGeAs_2$ samples a and b, while still lower than the 10 K band gap, appear at higher energy and are broader in linewidth than the normally observed DAP band near 0.52–0.59 eV for p-type $CdGeAs_2$ samples. For sample c, the origin of the band near 0.51 eV is most probably the DAP transition involving a shallow donor and the 120 meV acceptor. The peak of the 0.51 eV band shifted to higher energy with increasing laser power. The magnitude of the peak shift was about 15 meV when the power density changed by one order of magnitude. This variation in peak position with excitation power is similar to that attributed to the DAP recombination in p-type $CdGeAs_2$ [16]. The 0.51 eV peak energy is slightly lower than those for most p-type samples we have studied, which suggests that sample c is highly compensated with a larger magnitude of potential fluctuations than those typically found for as-grown p-type $CdGeAs_2$ samples. The temperature dependence of the 0.51 eV PL band from sample c also had similar behaviour to the higher energy PL band for p-type samples [16]. Thus, the higher energy band for sample c appears to be attributable to the same DAP recombination at 10 K as that for p-type samples containing large concentrations of the shallow 120 meV acceptor. Doping with indium donors did not suppress formation of the shallow acceptor in $CdGeAs_2$ grown by the HGF technique.

The near-edge PL band for the heavily In-doped samples is broad (see figure 1) and shifts to higher energy with increasing electron concentration. Band-to-band (B–B) [22–24], electron–acceptor [25], and DAP [26] transitions all have these features for highly doped semiconductors; thus it is often difficult to distinguish between these processes. Since we attribute the 0.51 eV PL band for sample c to DAP recombination, we compare the data for the

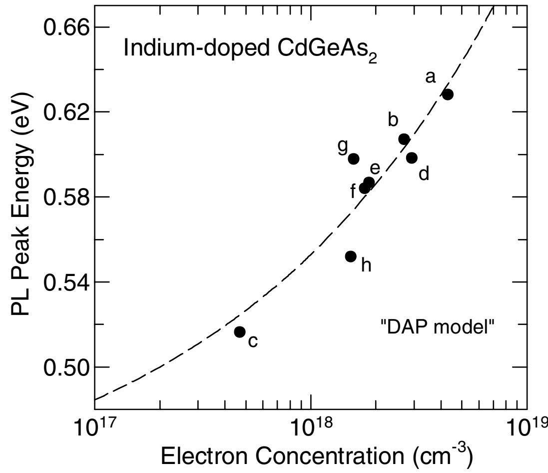

Figure 2. PL peak energy at 10 K versus room temperature electron concentration. The dashed line is the 'best fit' using equation (1) with $E_0 =$ 0.43 eV and $C = 1.3 \times 10^{-7}$ eV cm.

other In-doped samples with emission peaking above 0.5 eV to predictions for DAP in heavily doped materials. For DAP recombination in n-type material, the Coulomb interaction between the ionized donor and acceptor defects will increase with increasing donor concentration due to a decrease in pair separation distance. Assuming that the free electron concentration (n) scales with the donor concentration, the PL peak energy (E_{PL}) will vary as follows [26].

$$E_{PL} = E_0 + Cn^{1/3}. \tag{1}$$

Here, E_0 is the energy difference between the donor level and the acceptor level (i.e., $E_0 = E_g - E_D - E_A$). The parameter C is $e^2/2\pi\varepsilon_r\varepsilon_0$ (in SI units) assuming that the pair distance between the donor and acceptor varies as $r = \frac{1}{2}n^{-1/3}$. For $CdGeAs_2$, the relative dielectric constant ε_r is ~15 and the calculated value for C is 1.92×10^{-8} eV cm^{-1}.

Figure 2 shows the measured PL peak energy versus 300 K electron concentration for the eight In-doped $CdGeAs_2$ samples of our set having a PL band above 0.5 eV. For $CdGeAs_2$ at 300 K, the intrinsic carrier concentration is about 2.7×10^{13} cm^{-3}. The degenerate doping level for n-type material is about 1×10^{17} cm^{-3}. As shown in table 1, most of the doped samples included in our study have near to or above this concentration, so the error introduced in using the Hall measurement at 300 K for our PL analysis is assumed small. Also, we assume that the donor levels are shallow and that most are thermally ionized at 300 K. The dashed line is the best fit obtained using equation (1) and allowing both C and E_0 to vary. This approach gave $E_0 = 0.43$ eV and $C = 1.3 \times 10^{-7}$ eV cm. The E_0 value is much lower than the usual DAP energy value of ~0.55 eV for p-type material. Also, we can rule out the DAP model, as described using equation (1), because the parameter C obtained from the curve fit is one order higher than the calculated value.

A second possible origin of the peak shifts in PL for the heavily In-doped samples is the free-to-bound, or electron-to-acceptor (e, A^0) one. Effects of band filling, band gap shrinkage, and band tailing due to high doping concentrations in cubic materials have been reported [22–24]. Here, we include a nonzero crystal-field energy splitting when determining the nonparabolicity coefficient and make predictions for our n-type $CdGeAs_2$. Equation (2) gives the predicted PL transition energy for B–B recombination. For free-to-bound transitions, E_g is simply replaced with $E_g - E_A$. In equations (2)–(7), E_F^* is the Fermi energy corrected by considering nonparabolic bands, E_F^0 is the Fermi energy for parabolic bands relative to the bottom of the conduction band, E_c^{c*} is the band shift due to the electron–impurity interaction for screened Coulomb potentials and nonparabolic bands, E_c^c is the Coulomb energy term in

the case of parabolic bands, and E_c^e is the band gap shrinkage due to the exchange interaction between free carriers:

$$E_{PL} = E_g + E_F^* - E_c^{c*} - E_c^e \tag{2}$$

$$E_F^* = E_F^0\left(1 - \alpha\frac{E_F^0}{E_g}\right) \tag{3}$$

$$E_F^0 = \left(\frac{\hbar^2}{2m^*}\right)(3\pi^2 n)^{2/3} \tag{4}$$

$$E_c^{c*} = E_c^c\left(1 - 2\alpha\frac{E_F^0}{E_g}\right) \tag{5}$$

$$E_c^c = \left(\frac{\pi^{4/3}\hbar^2}{3^{1/3}}\right)\left(\frac{1}{m^*}\right)n^{2/3} \tag{6}$$

$$E_c^e = (e/2\pi\varepsilon_r\varepsilon_0)(3/\pi)^{1/3}n^{1/3} = \beta n^{1/3}. \tag{7}$$

In equation (7), the band gap shrinkage parameter β for $CdGeAs_2$ is 1.89×10^{-8} eV cm. The parameter α, used in equations (3) and (5), is a dimensionless nonparabolicity coefficient. Taking the conduction band density-of-states effective mass in $CdGeAs_2$ to be $m^* = 0.036\ m_0$ [27] and $\varepsilon_r = 15$, the calculation results give E_F^0 and E_c^c as a function of the free electron concentration in the following forms:

$$E_F^0 = 10.13 \times 10^{-14} n^{2/3}\ \text{eV} \tag{8}$$

$$E_c^c = 6.75 \times 10^{-14} n^{2/3}\ \text{eV}. \tag{9}$$

Next, we derive an expression for the nonparabolicity coefficient α, appropriate for our noncubic crystal structure. From the $\boldsymbol{k}\cdot\boldsymbol{p}$ method, we use the following equation from [27], which has been modified by assuming that the minimum conduction band of $CdGeAs_2$ is nearly isotropic:

$$E(E - E_1 - E_g)(E - E_1)(E - E_2) = \tfrac{1}{3}k^2P^2E(E + \tfrac{2}{3}\Delta_{so}) + \tfrac{2}{3}k^2P^2[(E - E_1)(E - E_2) - \tfrac{1}{3}\Delta_{so}(E + \Delta_{cf})] \tag{10}$$

where P is the momentum matrix element, Δ_{cf} is the crystal-field energy splitting, and Δ_{so} is the spin–orbit energy splitting. The energy values E_1 and E_2 are calculated from Δ_{so} and Δ_{cf}:

$$E_{1,2} = -\tfrac{1}{2}(\Delta_{so} + \Delta_{cf}) \pm \tfrac{1}{2}[(\Delta_{so} + \Delta_{cf})^2 - \tfrac{8}{3}\Delta_{so}\cdot\Delta_{cf}]^{1/2}. \tag{11}$$

For $CdGeAs_2$, $\Delta_{so} = 0.33$ eV, and $\Delta_{cf} = -0.21$ eV [1]; thus, $E_1 = 0.16$ eV and $E_2 = -0.29$ eV. If one assumes the simple form of a parabolic band, then the expression for the conduction band (relative to V_2) is

$$E_c = E_g + E_1 + \frac{(\hbar k)^2}{2m^*} \tag{12}$$

where E_g is the minimum band gap energy at $k = 0$, and m^* is the electron effective mass. For a nearly isotropic conduction band, E_c can also be written in terms of the free electron mass m and the matrix element P [27]:

$$E_c = E_g + E_1 + \frac{(\hbar k)^2}{2m} + \frac{k^2P^2}{3}\frac{E_g + E_1 + \frac{2}{3}\Delta_{so}}{E_g(E_g + E_1 - E_2)} + \frac{2k^2P^2}{3(E_g + E_1)}\left(1 - \frac{\Delta_{so}(E_g + E_1 + \Delta_{cf})}{3E_g(E_g + E_1 - E_2)}\right). \tag{13}$$

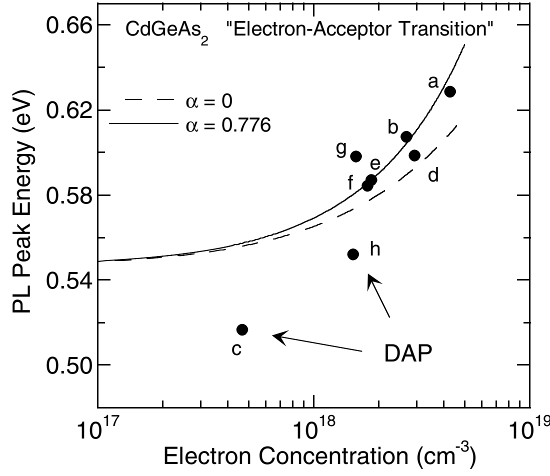

Figure 3. PL peak energy at 10 K versus room temperature electron concentration. The dashed line is the prediction for the electron–acceptor transition if band nonparabolicity is ignored. The solid line includes the nonparabolicity and is in better agreement with the data. The PL from samples c and h are assigned to DAP recombination and occur at lower energies. The acceptor level associated with these PL emissions is ~120 meV above the valence band.

From equations (12) and (13), an expression for P^2 is found:

$$P^2 = \frac{3\hbar^2}{2m^*}\left(1 - \frac{m^*}{m}\right)\frac{E_g(E_g + E_1 - E_2)(E_g + E_1)}{(E_g + E_1)^2 + 2E_g(E_g + E_1 - E_2) - \frac{2}{3}\Delta_{so}\Delta_{cf}}. \tag{14}$$

If the conduction band is nonparabolic and one keeps terms of order up to and including k^4, then the conduction band energy (relative to the top of V_2) is of the form [22, 23, 28]

$$E_c = E_g + E_1 + \frac{\hbar^2k^2}{2m^*} - \left(\frac{\alpha}{E_g}\right)\left(\frac{\hbar^2k^2}{2m^*}\right)^2 \tag{15}$$

where α, the nonparabolicity coefficient, is derived by substitution of $(E_c - h^2k^2/2m)$ into equation (10). For our case, the coefficient α can be expressed in terms of E_g, E_1, E_2, Δ_{cf}, and Δ_{so} as follows:

$$\alpha = \left(1 - \frac{m^*}{m}\right)^2\left[-\frac{\left(6 + 4\frac{E_1}{E_g} - 2\frac{E_2}{E_g}\right)}{\left(1 + \frac{E_1}{E_g}\right)^2 + 2\left(1 + \frac{E_1}{E_g} - \frac{E_2}{E_g}\right) - \frac{2}{3}\frac{\Delta_{so}}{E_g}\frac{\Delta_{cf}}{E_g}} + \frac{\left(1 + \frac{E_1}{E_g}\right)^2 + 2\left(1 + \frac{E_1}{E_g} - \frac{E_2}{E_g}\right) - \frac{E_1E_2}{E_g^2}}{\left(1 + \frac{E_1}{E_g}\right)\left(1 + \frac{E_1}{E_g} - \frac{E_2}{E_g}\right)}\right]. \tag{16}$$

In the limit of $\Delta_{cf} = 0$, our equations (14) and (16) reduce to expressions reported for cubic systems [29, 30]. Using a low temperature band gap energy of $E_g = 0.67$ eV, we find that $\alpha = 0.776$ for $CdGeAs_2$. This value for α is used in equations (3) and (5) and shifts in PL peak energy predicted for the free-to-bound recombination model can be compared to the data from the In-doped $CdGeAs_2$ samples.

Figure 3 shows the PL peak energies and the predicted free-to-bound transition energies for the shallow 120 meV acceptor in $CdGeAs_2$ assuming a parabolic conduction band (dashed line) or a nonparabolic band (solid line). The effect on the acceptor level of incorporation

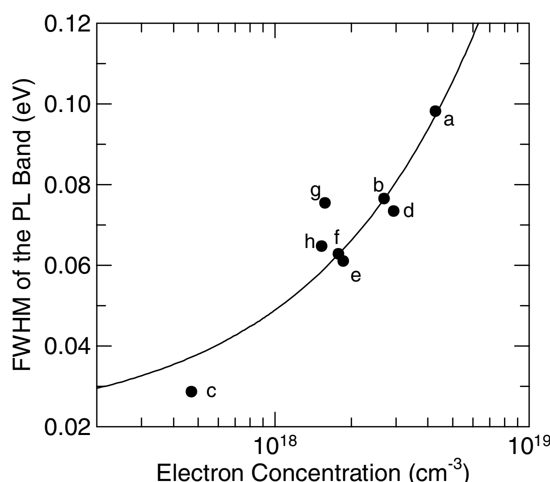

Figure 4. The FWHM of the 10 K PL band versus the 300 K electron concentration for the $CdGeAs_2$ samples doped heavily with indium. The solid line is a curve fit using equation (17).

of the donor dopant is assumed negligible. The free-to-bound transition energy is given by $E_g - E_A = (0.67 - 0.12)$ eV $= 0.55$ eV (call this E_{PL}) in the limit of an unperturbed band gap. This 120 meV acceptor energy is based on PL results obtained from p-type as-grown $CdGeAs_2$ [16]. Also, electrical activation energies of between 100 and 150 meV have been reported for as-grown p-type $CdGeAs_2$ [31]. The inclusion of α in our model gives predicted transition energies which are in excellent agreement with the PL peak energies for $n > 2 \times 10^{18}$ cm^{-3}. Because the donor/conduction band states are merged at high free carrier concentrations, the high energy PL band from the heavily In-doped n-type samples can be treated as arising from free-to-bound or electron-to-acceptor (e, A^0) recombination. Thus, we determine that bulk $CdGeAs_2$ samples grown by the HGF technique and containing large concentrations of indium donors still have the shallow acceptor defects, and it is these localized states that serve as the ground state for the radiative recombination.

The linewidth of the PL band from heavily In-doped $CdGeAs_2$ samples increased with electron concentration. The full width at half-maximum (FWHM) of the high energy PL band is plotted as a function of n in figure 4. Increases in PL linewidth due to an increase in Fermi level are often described by an $n^{2/3}$ power law [32]:

$$\mathrm{FWHM} = W_0 + kn^{2/3}. \tag{17}$$

The linewidths of the PL from the In-doped samples, especially at the higher concentrations, are well described by this power law. The solid line in figure 4 is a 'best fit' obtained using equation (17), and $W_0 = 0.019$ eV and $k = 2.9 \times 10^{-14}$ eV cm^2. This indicates that the line broadening for the In-doped samples is consistent with band filling.

Our study also included four $CdGeAs_2$ samples that were low n-type ($n < 10^{18}$ cm^{-3}). Surprisingly, the PL spectra for these four samples only had the one broad DAP band peaking near 0.35 eV due to shallow donors and deep 0.26 eV acceptors [11]. Two of the four samples, i and j, were cut from a boule doped with 10 ppm indium. This boule was grown along the [112] direction and, for undoped crystals, we have often seen improved sample transparency and only the deep-level PL band when this growth direction was used. Thus, large concentrations of the shallow 120 meV acceptor may not have been present in this material. The PL from these

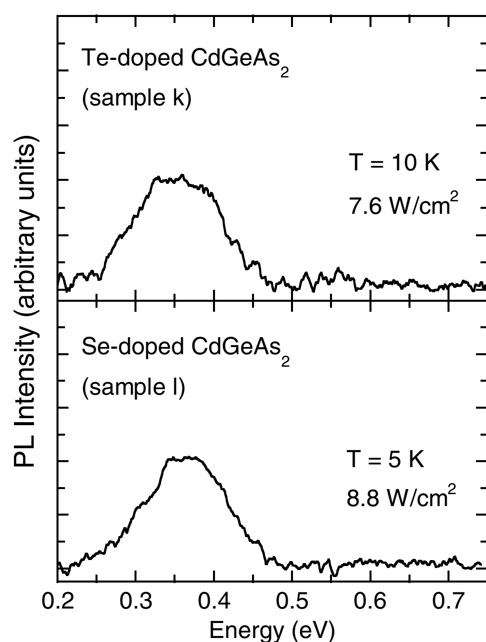

Figure 5. PL spectra from n-type $CdGeAs_2$ doped with Te (sample k) or Se (sample l).

two samples suggests that this low In doping level was not sufficient to suppress the deep-level band. The two other low n-type samples, k and l, were cut from boules doped with rather high concentrations of Te or Se, respectively. Figure 5 shows representative spectra obtained from these two samples. Group VI impurities, such as the Te and Se used here, will act as singly ionized donors when incorporated on the anion site in $CdGeAs_2$. Thus, it is tempting to consider that doping on the As site will affect the formation of the shallow Ge_{As} native defect during growth. As a result, the DAP recombination or electron–acceptor recombination associated with Ge_{As} acceptors could be reduced or eliminated entirely. Although this is consistent with the experimental result (i.e., no high energy PL band), it is still possible that the concentrations of Ge_{As} acceptors were initially low to begin with in these samples due to other growth factors. Further studies on a larger sample set are necessary in order to associate suppression of the shallow Ge_{As} acceptor with anion site doping.

4. Conclusion

The PL from n-type $CdGeAs_2$ crystals doped with indium, selenium, or tellurium can be used to determine which acceptor states are present. In samples heavily doped with indium, the PL band related to the deep native acceptor is absent, while the shifts in energy of the near-edge PL are shown to be consistent with (e, A^0) recombination associated with the shallow 120 meV acceptor level (previously attributed to Ge_{As}). In our analysis, band filling, band tailing, and band shrinkage effects were accounted for, and an expression was derived for describing the nonparabolicity of the conduction band for nonzero Δ_{cf}. For Se- and Te-doped samples, the PL due to the shallow acceptor level is absent, although the deep-level PL is still observed. The absence of the deep acceptor in highly indium-doped samples suggests that doping on the group II site is particularly effective in eliminating this defect. Our PL data suggest that the deep acceptor may be an isolated Cd vacancy or a point defect complex involving this vacancy.

Acknowledgments

The authors wish to thank R C DeMattei for help with the growth experiments at Stanford University. The work at West Virginia University and Stanford University was supported by the Air Force Office of Scientific Research under grant number F49620-01-1-0428.

References

[1] Shileika A 1973 *Surf. Sci.* **37** 730
[2] Akimchenko I P, Borshchevskii A S and Ivanov V S 1973 *Sov. Phys.—Semicond.* **7** 98
[3] Schunemann P G and Pollak T M 1997 *J. Cryst. Growth* **174** 272
[4] Schunemann P G and Pollak T M 1997 Method for growing crystals *US Patent Specification* 5,611,856
[5] Schunemann P G and Pollak T M 1998 *Mater. Res. Soc. Bull.* **23** 23
[6] Schunemann P G, Setzler S D, Pollak T M, Ptak A J and Myers T H 2001 *J. Cryst. Growth* **225** 440
[7] Schunemann P G and Pollak T M 1998 *Mater. Res. Soc. Bull.* **23** 1096
[8] Zakel A, Blackshire J L, Schunemann P G, Setzler S D, Goldstein J and Guha S 2002 *Appl. Opt.* **41** 2299
[9] Vodopyanov K L and Schunemann P G 1998 *Opt. Lett.* **23** 1096
[10] Vodopyanov K L, Knippels G M H, Van der Meer A F G, Maffetone J P and Zwieback I 2002 *Opt. Commun.* **202** 205
[11] Bai L, Giles N C and Schunemann P G 2005 *J. Appl. Phys.* **97** 023105
[12] Mamedov B Kh and Osmanov É O 1972 *Sov. Phys.—Semicond.* **5** 1120
[13] McCrae J E, Hengehold R L, Yeo Y K, Ohmer M C and Schunemann P G 1997 *Appl. Phys. Lett.* **70** 455
[14] Aufgang J B, Labrie D, Olsen K, Paton B, Simpson A M, Iseler G W and Borshchevsky A 1997 *Semicond. Sci. Technol.* **12** 1257
[15] Bai L, Poston J A Jr, Schunemann P G, Nagashio K, Feigelson R S and Giles N C 2004 *J. Phys.: Condens. Matter* **16** 1279
[16] Bai L, Giles N C, Schunemann P G, Pollak T M, Nagashio K and Feigelson R S 2004 *J. Appl. Phys.* **95** 4840
[17] Bai L, Garces N Y, Yang N, Schunemann P G, Setzler S D, Pollak T M, Halliburton L E and Giles N C 2003 *Mater. Res. Soc. Proc.* **744** 537
[18] Blanco Miguel A, Costales A, Luana V and Pandey R 2004 *Appl. Phys. Lett.* **85** 4376
[19] Borshchevskii A S, Goryunova N A, Osmanov E O, Polushina I K, Royenkov N D and Smirnova A D 1968/1969 *Mater. Sci. Eng.* **3** 118
[20] Bairamov B H, Rud V Yu and Rud Yu V 1998 *Mater. Res. Soc. Bull.* **23** 41
[21] Nagashio K, Watcharapasorn A, Zawilski K T, DeMattei R C, Feigelson R S, Bai L, Giles N C, Halliburton L E and Schunemann P G 2004 *J. Cryst. Growth* **269** 195
[22] Bugajski M and Lewandowski W 1985 *J. Appl. Phys.* **57** 521
[23] Yoon I T, Ji T S, Oh S J, Choi J C and Park H L 1997 *J. Appl. Phys.* **82** 4024
[24] Levy M, Lee W K, Sarachik M P and Geschwind S 1992 *Phys. Rev.* B **45** 11685
[25] Zemon S, Vassell M O, Lambert G and Bartram R H 1982 *J. Appl. Phys.* **53** 3347
[26] As D J, Richter A, Busch J, Schottker B, Lubbers M, Mimkes J, Schikora D, Lischka K, Kriegseis W, Burkhardt W and Meyer B K 2000 *Mater. Res. Soc. Proc.* **595** W3.81.1
[27] Kildal H 1974 *Phys. Rev.* B **10** 5082
[28] Raymond A, Robert J L and Bernard C 1979 *J. Phys. C: Solid State Phys.* **12** 2289 (note that these authors use $\hbar^2 p^2$ for P^2)
[29] Irikawa M, Ishikawa T, Sasaki Y, Iwasawa K, Suemune I and Iga K 1998 *J. Appl. Phys.* **84** 4667 (the authors give P^2 in their equation A18)
[30] Hiroshima T and Lang R 1986 *Appl. Phys. Lett.* **49** 456 (the authors define a nonparabolicity in their equation (5) using $\gamma = \alpha(\hbar^2/(2m^* E_g))$, where α is our nonparabolicity coefficient)
[31] Fischer D W, Ohmer M C and McCrae J E 1997 *J. Appl. Phys.* **81** 3579
[32] Yoshikawa M, Kunzer M, Wagner J, Obloh H, Schlotter P, Schmidt R, Herres N and Kaufmann U 1999 *J. Appl. Phys.* **86** 4400